275 nm Deep Ultraviolet AlGaN-Based Micro-LED Arrays for Ultraviolet Communication

Liang Guo, Yanan Guo, Jiankun Yang, Jianchang Yan, Jianguo Liu, Junxi Wang, and Tongbo Wei

***Abstract*—In this work, we fabricated and characterized 4 × 4 parallel flip-chip AlGaN-based micro-LED arrays with varied mesa diameters of 120 μm, 100 μm, 80 μm, and 60 μm. The reported micro-LED arrays have a maximum bandwidth of 380 MHz and a peak wavelength of ∼275 nm. It is found that the electrical and optical characteristics of AlGaN-based micro-LED arrays show strong size dependence for ultraviolet communication (UVC). The differential resistance increases from 28.8 Ω to 112 Ω, the external quantum efficiency (EQE) is increased by ∼30%, and the bandwidth doubles as the diameter of individual micro-LED decreases from 120 μm to 60 μm. Our research proves that tailoring the mesa size of parallel flip-chip AlGaN-based micro-LED arrays can further enhance its bandwidth and promote its application in UVC.**

***Index Terms*—Micro-LED arrays, ultraviolet communication, modulation bandwidth, size dependence.**

I. Introduction

RECENTLY, ultraviolet communication (UVC) has emerged as a promising candidate for military wireless communication [1], [2]. Record-breaking data rate has been reported continuously in the past few years[3]–[6]. Compared to its visible-light counterparts, UVC has several unique features. The light used in the UVC is located between 200 nm ∼ 280 nm in the spectrum band. This portion of solar radiation is heavily absorbed by the ozone layer when passing through the atmosphere, leaving low noise background near the ground [7]. Visible light communication (VLC) usually requires an obstacle-free communication channel between transceivers while the ultraviolet light signal in UVC can bypass obstacles through scattering and reflection of the particles and aerosols floating in the air [8], [9]. Furthermore, the quickly attenuated ultraviolet radiation will limit the transmission range of UVC and prevent eardrop from a distance [3]. In radio-silent scenarios, UVC can work as an alternative to conventional wireless communication.

Deep ultraviolet (DUV) light source is one of the most critical components of the UVC system. Its optical power essentially determines transmission distance of UVC, and its bandwidth has a major impact on the data rate [10]. More and more UVC research has adopted LEDs as the light sources due to their high efficiency, portable size, tunable emission range, and high bandwidth [11], [12]. Recently, Alkhazragi *et al.* demonstrated a 2.4 Gbps communication system over a 1 m link based on a 278 nm DUV LED with a −3 dB bandwidth of 170 MHz [4]. When the transmission distance is further increased to 5 m, a data rate of 2.0 Gbps still maintained. They also conducted a series of experiments on diffuse line-of-sight (diffuse-LOS) UVC based on the same DUV LED, achieving up to 1.09 Gbps data rate [6]. In 2018, Kojima *et al.* achieved a 1.6 Gbps data rate over a 1.5 m LOS link based on a 280 nm LED with a −3 dB bandwidth of 153 MHz [5]. Despite all the exceptional results above, the data rate of UVC is still largely limited by the modulation bandwidth of DUV LED. The community is still in the exploration of new approaches to boost DUV LED's modulation bandwidth.

In the past years, it has found that InGaN-based LEDs in VLC show remarkable improvement on both optical characteristics and modulation bandwidth when reducing the chip size to the micro range [13]–[19]. Micro-LEDs can work under much higher current density due to uniform current spreading and quick heat dissipation. Higher current density and smaller chip size lead to lower carrier lifetime and resistance-capacitance time constant, both of which can boast a higher bandwidth for micro-LED. All the above advantages can also render AlGaN micro-LED an ideal light source for UVC. The latest research has witnessed a drastic increase in micro-LED properties for UVC application. In 2020, He *et al.* used a 262 nm micro-LED with a bandwidth of 438 MHz at a current density of 71 A/cm^2 as the light source, achieving up to 1.1 Gbps data transmission rate over 0.3 m UVC link [20]. In 2021, Zhu *et al.* achieved a record-breaking data rate of 2 Gbps over 0.5 m UVC link with a 276.8 nm micro-LED [21]. The reported micro-LED obtained a record-high −3 dB optical bandwidth of 452.53 MHz at a current density of 400 A/cm^2. The size effect on electro-optic properties of AlGaN-based individual micro-LED has been reported by Yu et al [22]. However, the size effect on the electro-optic properties of AlGaN-based micro-LED arrays which contains multiple individual micro-LEDs remains relatively unexplored.

Manuscript received November 11, 2021; accepted November 18, 2021. Date of publication November 22, 2021; date of current version December 5, 2021. This work was supported in part by the National Key R&D Program of China under Grants 2017YFB0404104 and 2019YFA0708203, in part by the National Natural Science Foundation of China under Grant 61974139, and in part by Beijing Natural Science Foundation under Grant 4182063. *(Corresponding author: Jianguo Liu; Tongbo Wei.)*

Liang Guo, Yanan Guo, Jiankun Yang, Jianchang Yan, Junxi Wang, and Tongbo Wei are with the Research and Development Center for Semiconductor Lighting Technology, Institute of Semiconductors, Chinese Academy of Sciences, Beijing 100083, China (e-mail: guoliang18@semi.ac.cn; ynguo@semi.ac.cn; yjkun@semi.ac.cn; yanjc@semi.ac.cn; jxwang@semi.ac.cn; tbwei@semi.ac.cn).

Jianguo Liu is with the Center of Materials Science and Optoelectronics Engineering, University of Chinese Academy of Sciences, Beijing 100049, China, and also with the State Key Laboratory of Integrated Optoelectronics, Institute of Semiconductors, Chinese Academy of Sciences, Beijing 100083, China (e-mail: jgliu@semi.ac.cn).

Digital Object Identifier 10.1109/JPHOT.2021.3129648

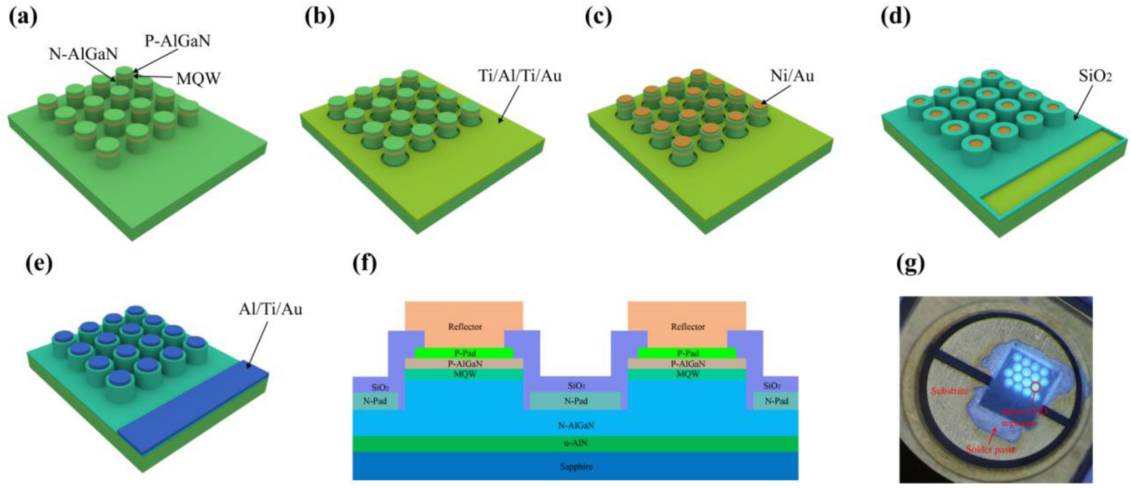

Fig. 1. (a–e) Schematic diagrams of the fabrication process for 4 × 4 parallel flip-chip AlGaN-based micro-LED arrays. (f) The schematic structure of the pixels in the micro-LED arrays. (g) 120 μm micro-LED arrays bonded on a metalized substrate.

Compared to individual micro-LED, micro-LED arrays have the potential of reaching higher optical power, and also enable the high bandwidth of micro-LED, making micro-LED arrays more ideal candidate for long distance high speed communication. Moreover, there is still a knowledge gap about the relation between the chip size and modulation characteristics of AlGaN-based micro-LED.

In this work, we experimentally investigate 4 × 4 parallel flip-chip AlGaN-based micro-LED arrays with varied mesa diameters. In order to attain higher optical power for the investigation of modulation characteristics, the mesa diameter is set to be 120 μm, 100 μm, 80 μm, and 60 μm respectively. The reported micro-LED arrays demonstrate a maximum bandwidth of 380 MHz with a peak wavelength of ∼275 nm at the current density of 10 A/cm^2. It is found that the electrical and optical characteristics of AlGaN-based micro-LED arrays show strong size dependence. The differential resistance increases from 28.8 Ω to 112 Ω and the external quantum efficiency (EQE) is increased by nearly 30% as the diameter of individual micro-LED decreases from 120 μm to 60 μm. The bandwidth of the micro-LED arrays nearly double from 174 MHz to 380 MHz as the mesa diameter decreases. The present research detailedly explores the effects of mesa size on the electro-optic characteristics and modulation bandwidth of the AlGaN-based micro-LED arrays.

II. Device Fabrication

The 275 nm DUV LED epitaxial wafer used in this work was grown on a sapphire substrate including mainly a 2.5 μm AlN buffer layer, 500 nm thick unintentional doped AlGaN layer, 1.5 μm thick n-doped $Al_{0.55}Ga_{0.45}N$ layer, 5 period AlGaN multiple quantum wells (MQWs), and 70 nm thick p-doped $Al_{0.5}Ga_{0.5}N$ layer. Conventional visible LEDs are usually lateral structure. However, due to the lack of transparent p-contact, DUV micro-LED arrays in our work are fabricated as flip-chip structure instead. As depicted in Fig. 1(a)-(e), the fabrication process is similar to our previous works [23], [24]. Standard photolithography and inductively coupled plasma (ICP) etching were utilized to form mesa with the diameter of 120 μm, 100 μm, 80 μm, and 60 μm, respectively. Then n-electrodes composed of Ti/Al/Ti/Au (20 nm/60 nm/30 nm/100 nm) were deposited on the mesa after photolithography. Rapid thermal annealing (RTA) at 1000°C was employed to form the Ohmic n-contact. P-electrodes of Ni/ Au (20 nm/20 nm) were deposited on the p-AlGaN and rapidly annealed at 700°C to form the Ohmic p-contact. An 1100-nm-thick SiO_2 was deposited as the insulting layer using plasma-enhanced chemical vapor deposition (PECVD) followed by photolithography, reactive ion etching (RIE), and wet etching to form SiO_2 apertures. Furthermore, an Al/Ti/Au (1700 nm/50 nm/300 nm) layer is deposited on electrodes as a reflector. The schematic structure of the pixels in the micro-LED arrays was shown in Fig. 1(f). Micro-LED arrays were bonded on a metalized substrate as shown in Fig. 1(g). Broad-area flip-chip DUV LEDs using the same fabrication process with active region area of 1.53×10^{-3} cm^2 which falls in between that of 120 μm micro-LED arrays (1.81×10^{-3} cm^2) and 100 μm micro-LED arrays (1.26×10^{-3} cm^2) were also fabricated for the reference. Electrical and optical measurements of the packaged devices were carried out using a calibrated integrating sphere (Everfine HAAS-2000).

III. Results and Analysis

Fig. 2(a) shows the I–V characteristics of different micro-LED arrays and broad area LED. We can extract the differential resistance under the current of 20 mA. The resistance increases from 28.8 Ω to 112 Ω when the diameter of individual micro-LED decreases from 120 μm to 60 μm as shown in Fig. 2(b). Assuming the current distributes evenly in the p-AlGaN layer, the resistance of individual micro-LED can be described as [22], [25]:

$$R = 4\rho d/\pi D^2 + R_c \tag{1}$$

where R_c is the contact resistance derived from Ohmic contact between electrodes and wafer. $4\rho d/\pi D^2$ is the series resistance of the mesa which consists of p-AlGaN, MQWs, and n-AlGaN. The ρ, d, D represents mesa's overall resistivity, thickness, and diameter. It can be seen that the series resistance is proximately

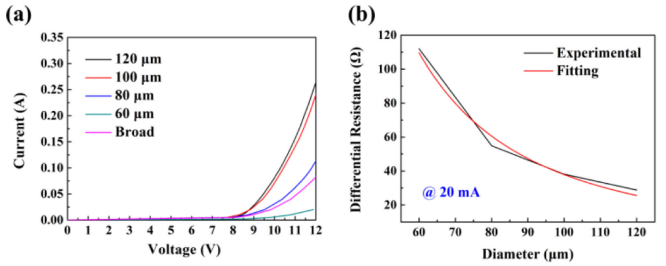

Fig. 2. (a) I–V characteristics of the micro-LED arrays with diameters of 120, 100, 80, and 60 μm and broad-area LEDs. (b) The extracted differential resistance of the micro-LED arrays from I–V curves under 20 mA.

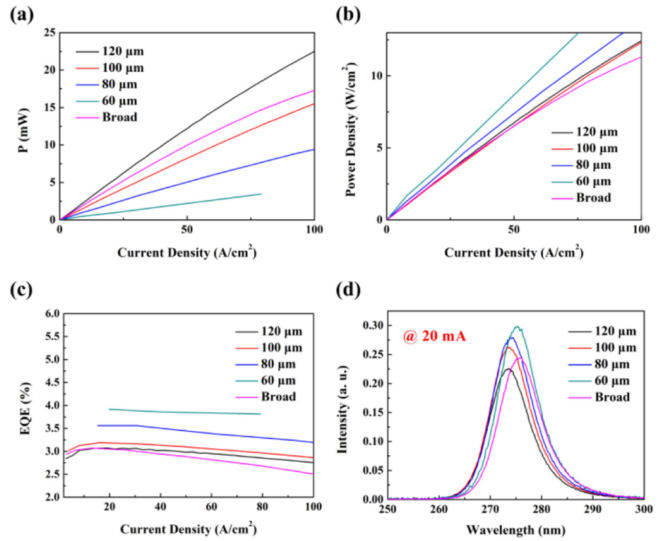

Fig. 3. (a) The optical power and (b) optical power density and (c) EQE against current density for the 120, 100, 80, and 60 μm micro-LED arrays and broad-area LED. (d) EL spectra for the 120, 100, 80, and 60 μm micro-LED arrays and broad-area LED measured at 20 mA.

proportional to the D^{-2}, indicating that reducing the mesa diameter will boast higher resistance for micro-LEDs, which is consistent with our experimental results.

Fig. 3(a) demonstrates the optical power of micro-LED arrays and their broad area counterpart under different injection current densities. The optical power increases monotonously as the chip size increases. As plotted in Fig. 3(b), the optical power density of micro-LED arrays shows evident size dependence. This is because reducing the chip size can alleviate photon's reflection from mesa and minimize the path loss, leading to higher optical power density [26]. This explanation is also confirmed by EQE under different current densities, as shown in Fig. 3(c). EQE is expressed as follow[27]:

$$EQE = q\lambda P/Ihc \tag{2}$$

In the above expression, q is the elementary charge, λ is the peak wavelength, P is the optical output power, I is the current, h is the Planck's constant, and c is the light speed in a vacuum. We can conclude that a smaller mesa size can help increase the light extraction from micro-LED arrays and give rise to higher EQE. Additionally, all micro-LED arrays, regardless of their mesa size, appear to display higher power density and EQE compared to broad area LED. This is due to the reason that microstructures in micro-LED arrays can serve as the roughened surfaces and reduces internal light reflection and scatters the light outward [24], [28]. The partial strain relaxation in the microstructures also helps reduce the Quantum-confined stark effect (QCSE) in the MQWs and boosts radiation combination [29].

Electroluminescent (EL) spectra measured under 20 mA are shown for Micro-LED arrays and broad-area LED in Fig. 3(d). We can observe a 0.5∼2.3 nm blue shift of peak wavelength and narrowing full-width at half-maximum (FWHM) on micro-LEDs arrays, as compared to broad-area LEDs. This is mainly attributed to the partial strain relaxation in the microstructures which alleviates the QCSE in the MQWs [29], [30]. Nevertheless, an evident red-shift of the peak wavelength can be observed as the diameter of individual micro-LED decreases. This discrepancy could be attributed to the self-heating under different current densities [31]. That is, the smaller the chip size is, the larger current density will be under the same current, which will generate more heat in a unit time and increase chip temperature [32]. The increased temperature will thus reduce the bandgap of the micro-LED. The temperature-dependent bandgap energy $E_g(T)$ can be expressed as a linear approximation as the following expression [33]:

$$E_g\,(T) = E_0 - pkT \tag{3}$$

where E_0 represents the linearly extrapolated band-gap energy at 0 K, and p is a positive constant defining the bandgap shift of an LED as a function of temperature, k is the Boltzmann constant. Narrower bandgap will lead to longer wavelength for LED according to Planck-Einstein relation:

$$E = hc/\lambda \tag{4}$$

To investigate the modulation bandwidth of the micro-LED arrays, a vector network analyzer (Agilent E5061B) is used to generate an alternating current (AC) frequency sweep signal and added to a direct current (DC) bias tee driven by DC supply (Keithley 2400). The combined signal is then delivered to micro-LED arrays to generate the light signal. A Si-based APD (Thorlabs APD430A2/M) is used as the detector in this work. A filter is used to block the visible light that might interfere with the measurement. The output signal of the detector is sent back to the network analyzer to calculate the frequency response. High-frequency cables and adaptors are used to connect the radio frequency (RF) equipment. The experimental setup of the test system is shown in Fig. 4.

The frequency response of micro-LEDs under the current density of 10 A/cm^2 is measured and normalized as shown in Fig. 5(a). The extracted modulation bandwidths (-3 dB) for 120 μm, 100 μm, 80 μm and 60 μm micro-LED arrays are 174, 190, 325, and 380 MHz, respectively. Micro-LED arrays with smaller chip size appear to have larger modulation bandwidth at the same current density. It is noted that the -3 dB bandwidth nearly doubles as the diameter decreases from 120 μm to 60 μm as shown in Fig. 5(b). Carrier lifetime can be seen as consistent in all sizes of micro-LED arrays when current density is fixed,

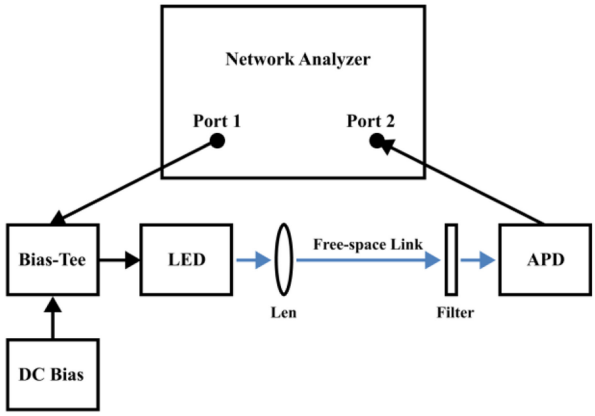

Fig. 4. The experimental setup of the UVC test system.

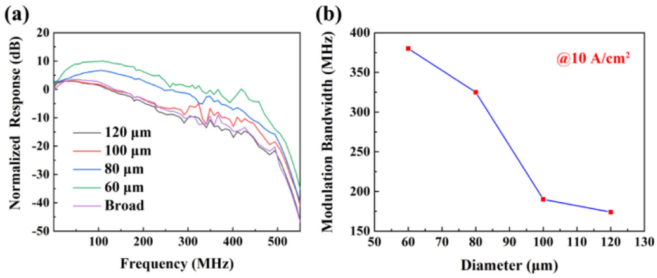

Fig. 5. (a) Frequency responses and (b) bandwidth of the 120, 100, 80, and 60 μm micro-LED arrays.

according to the following expression [34]:

$$\tau = \frac{-BP_0qd + \sqrt{(BP_0qd)^2 + 4BJqd}}{2BJ} \tag{5}$$

where τ is the carrier lifetime, B is the bimolecular coefficient, P_0 is the hole concentration, J is the injection current density, q is the elementary charge, and d is the thickness of the active layer. When LED is forward biased, the device capacitance is mainly affected by the diffusion capacitance and depletion-layer capacitance [35]. However, the depletion-layer capacitance is very small compared to the diffusion capacitance. Hence, depletion-layer capacitance is neglected in forward biased diode. Diffusion capacitance can be expressed as follow:

$$C_{diff} = qI\tau/2KT \tag{6}$$

Where q is the elementary charge, I is the forward bias current, τ is the minority carrier's lifetime, K is Boltzmann constant, and T is the thermodynamic temperature [34]. The micro-LED arrays in our work are in parallel connection. Thus, the overall capacitance of the micro-LED arrays will be the sum of individual pixel's capacitance. When the current density is fixed, current changes proportionally to the chip size, leading to larger diffusion capacitance and lower modulation bandwidth for larger size of chips [34], [36]. Although the resistance variation for different sizes of micro-LED arrays contradicts this trend, the bandwidth of LED chips is mainly influenced by the carrier lifetime and capacitance. The decrease of capacitance has more impact on the bandwidth than the increase of resistance [34]. The modulation bandwidth for broad area LED with active region area between 120 μm and 100 μm micro-LED arrays is measured to be 188 MHz, which falls in between the modulation bandwidth of 120 μm and 100 μm DUV micro-LED arrays. This result is well consistent with our previous analysis.

IV. Conclusion

In summary, we successfully fabricated 4 × 4 parallel flip-chip AlGaN-based micro-LED arrays with varied mesa diameters of 120 μm, 100 μm, 80 μm, and 60 μm. The optical power increase monotonously as the mesa diameter increases. The differential resistance shows a nearly 4-fold increase and the EQE is increased by nearly 30% as the diameter of individual micro-LED decreases from 120 μm to 60 μm. Operated at 10 A/cm^2 the bandwidth of the micro-LED arrays nearly double from 174 MHz to 380 MHz as the mesa diameter decreases from 120 μm to 60 μm. Moreover, compared to the broad-area LED, the peak wavelength of micro-LED arrays shows an evident blue shift, and the peak wavelength of micro-LED arrays also shows a redshift as the mesa diameter decreases. Our research paves the way for the future application of AlGaN-based micro-LED arrays in UVC and offer valuable insight into the understanding of the electrical and optical characteristic of AlGaN-based micro-LED arrays.

References

[1] Z. Xu and B. M. Sadler, "Ultraviolet communications: Potential and state-of-the-art," *IEEE Commun. Mag.*, vol. 46, no. 5, pp. 67–73, May 2008.
[2] G. A. Shaw, A. M. Siegel, J. Model, and D. Greisokh, "Recent progress in short-range ultraviolet communication," in *Proc. Int. Soc. for Opt. Photon.*, Orlando, FL, USA, Mar. 2018, pp. 214–225.
[3] A. Vavoulas, H. G. Sandalidis, N. D. Chatzidiamantis, Z. Xu, and G. K. Karagiannidis, "A survey on ultraviolet C-band (UV-C) communications," *IEEE Commun. Surv. Tut.*, vol. 21, no. 3, pp. 2111–2133, Feb. 2019.
[4] O. Alkhazragi *et al.*, "2.4-Gbps ultraviolet-C solar-blind communication based on probabilistically shaped DMT modulation," in *Proc. Opt. Fiber Commun. Conf.*, San Diego, CA, USA, Mar. 2020, pp. 1–3.
[5] K. Kojima *et al.*, "1.6-Gbps LED-based ultraviolet communication at 280 nm in direct sunlight," in *Proc. Eur. Conf. Opt. Commun.*, Rome, Italy, Sep. 2018, pp. 1–3.
[6] O. Alkhazragi *et al.*, "Gbit/s ultraviolet-C diffuse-line-of-sight communication based on probabilistically shaped DMT and diversity reception," *Opt. Exp.*, vol. 28, no. 7, pp. 9111–9122, 2020.
[7] R. J. Drost and B. M. Sadler, "Survey of ultraviolet non-line-of-sight communications," *Semicond. Sci. Technol.*, vol. 29, no. 8, Jun. 2014, Art. no. 084006.
[8] H. Ding, G. Chen, A. K. Majumdar, B. M. Sadler, and Z. Xu, "Modeling of non-line-of-sight ultraviolet scattering channels for communication," *IEEE J. Sel. Areas Commun.*, vol. 27, no. 9, pp. 1535–1544, Dec. 2009.
[9] P. Wang and Z. Xu, "Characteristics of ultraviolet scattering and turbulent channels," *Opt. Lett.*, vol. 38, no. 15, pp. 2773–2775, Jul. 2013.
[10] L. Guo, Y. Guo, J. Wang, and T. Wei, "Ultraviolet communication technique and its application," *J. Semicond.*, vol. 42, no. 8, Aug. 2021, Art. no. 081801.
[11] Y. Muramoto, M. Kimura, and S. Nouda, "Development and future of ultraviolet light-emitting diodes: UV-LED will replace the UV lamp," *Semicond. Sci. Technol.*, vol. 29, no. 8, Jun. 2014, Art. no. 084004.
[12] M. Akhter *et al.*, "Over 20 MHz modulation bandwidth on 250 nm emission of AlGaN micro-LEDs," *Electron. Lett.*, vol. 51, no. 4, pp. 354–355, Feb. 2015.
[13] S. Chen *et al.*, "High-bandwidth green semipolar (20–21) InGaN/GaN micro light-emitting diodes for visible light communication," *ACS Photon.*, vol. 7, no. 8, pp. 2228–2235, Jul. 2020.

[14] R. X. Ferreira *et al.*, "High bandwidth GaN-based micro-LEDs for multi-Gb/s visible light communications," *IEEE Photon. Technol. Lett.*, vol. 28, no. 19, pp. 2023–2026, Jun. 2016.

[15] J. J. McKendry *et al.*, "High-speed visible light communications using individual pixels in a micro light-emitting diode array," *IEEE Photon. Technol. Lett.*, vol. 22, no. 18, pp. 1346–1348, Jul. 2010.

[16] H.-Y. Lan, I.-C. Tseng, Y.-H. Lin, G.-R. Lin, D.-W. Huang, and C.-H. Wu, "High-speed integrated micro-LED array for visible light communication," *Opt. Lett.*, vol. 45, no. 8, pp. 2203–2206, Apr. 2020.

[17] R. Lin, X. Liu, G. Zhou, Z. Qian, X. Cui, and P. Tian, "InGaN Micro-LED array enabled advanced underwater wireless optical communication and underwater charging," *Adv. Opt. Mater.*, vol. 9, Apr. 2021, Art. no. 2002211.

[18] Y. H. Chang *et al.*, "High-bandwidth InGaN/GaN semipolar micro-LED acting as a fast photodetector for visible light communications," *Opt. Exp.*, vol. 29, no. 23, pp. 37245–37252, Oct. 2021.

[19] K. J. Singh *et al.*, "Micro-LED as a promising candidate for high-speed visible light communication," *Appl. Sci.*, vol. 10, no. 20, Oct. 2020, Art. no. 7384.

[20] X. He *et al.*, "1 Gbps free-space deep-ultraviolet communications based on III-nitride micro-LEDs emitting at 262 nm," *Photon. Res.*, vol. 7, no. 7, pp. B41–B47, Jun. 2019.

[21] S. Zhu *et al.*, "2 Gbps free-space ultraviolet-C communication based on a high-bandwidth micro-LED achieved with pre-equalization," *Opt. Lett.*, vol. 46, no. 9, pp. 2147–2150, Apr. 2021.

[22] H. Yu *et al.*, "AlGaN-based deep ultraviolet micro-LED emitting at 275 nm," *Opt. Lett.*, vol. 46, no. 13, pp. 3271–3274, Jun. 2021.

[23] H. Chang *et al.*, "Quasi-2D growth of aluminum nitride film on graphene for boosting deep ultraviolet light-emitting diodes," *Adv. Sci.*, vol. 7, no. 15, Jun. 2020, Art. no. 2001272.

[24] Y. Guo *et al.*, "Light extraction enhancement of ALGaN-based ultraviolet light-emitting diodes by substrate sidewall roughening," *Appl. Phys. Lett.*, vol. 111, no. 1, Jul. 2017, Art. no. 011102.

[25] A. Mohsen, Q. Li, M. Sachdev, and W. Wong, "Size-dependent optoelectrical properties of 365 nm ultraviolet light-emitting diodes," *Nanotechnology*, vol. 30, no. 50, Sep. 2019, Art. no. 504001.

[26] H. Choi, C. Jeon, M. Dawson, P. Edwards, R. Martin, and S. Tripathy, "Mechanism of enhanced light output efficiency in InGaN-based micro-light emitting diodes," *J. Appl. Phys.*, vol. 93, no. 10, pp. 5978–5982, May 2003.

[27] R. T. Ley *et al.*, "Revealing the importance of light extraction efficiency in InGaN/GaN microLEDs via chemical treatment and dielectric passivation," *Appl. Phys. Lett.*, vol. 116, no. 25, Jun. 2020, Art. no. 251104.

[28] T. Fujii, Y. Gao, R. Sharma, E. Hu, S. DenBaars, and S. Nakamura, "Increase in the extraction efficiency of GaN-based light-emitting diodes via surface roughening," *Appl. Phys. Lett.*, vol. 84, no. 6, pp. 855–857, Feb. 2004.

[29] L. Dai, B. Zhang, J. Lin, and H. Jiang, "Comparison of optical transitions in InGaN quantum well structures and microdisks," *J. Appl. Phys.*, vol. 89, no. 9, pp. 4951–4954, Apr. 2001.

[30] T. Wang, D. Nakagawa, J. Wang, T. Sugahara, and S. Sakai, "Photoluminescence investigation of InGaN/GaN single quantum well and multiple quantum well," *Appl. Phys. Lett.*, vol. 73, no. 24, pp. 3571–3573, Dec. 1998.

[31] Z. Gong *et al.*, "Size-dependent light output, spectral shift, and self-heating of 400 nm InGaN light-emitting diodes," *J. Appl. Phys.*, vol. 107, no. 1, Jan. 2010, Art. no. 013103.

[32] S. Lu *et al.*, "Low thermal-mass LEDs: Size effect and limits," *Opt. Exp.*, vol. 22, no. 26, pp. 32200–32207, Dec. 2014.

[33] H. Baumgartner, A. Vaskuri, P. Kärhä, and E. Ikonen, "Temperature invariant energy value in LED spectra," *Appl. Phys. Lett.*, vol. 109, no. 23, Dec. 2016, Art. no. 231103.

[34] Y. Huang, Z. Guo, H. Huang, and H. Sun, "Influence of current density and capacitance on the bandwidth of VLC LED," *IEEE Photon. Technol. Lett.*, vol. 30, no. 9, pp. 773–776, Mar. 2018.

[35] Y. Huang, Z. Guo, X.. Wang, H. Li, and D. Xiang, "GaN-based high-response frequency and high-optical power matrix micro-LED for visible light communication," *IEEE Electron Device Lett.*, vol. 41, no. 5, pp. 1536–1539, Apr. 2020.

[36] C.-L. Liao, C.-L. Ho, Y.-F. Chang, C.-H. Wu, and M.-C. Wu, "High-speed light-emitting diodes emitting at 500 nm with 463-MHz modulation bandwidth," *IEEE Electron Device Lett.*, vol. 35, no. 5, pp. 563–565, Apr. 2014.